

UC Davis

UC Davis Previously Published Works

Title

Structure and Reactivity of X-ray Amorphous Uranyl Peroxide, U₂O₇.

Permalink

<https://escholarship.org/uc/item/51x8b33k>

Journal

Inorganic chemistry, 55(7)

ISSN

0020-1669

Authors

Odoh, Samuel O
Shamblin, Jacob
Colla, Christopher A
[et al.](#)

Publication Date

2016-04-01

DOI

10.1021/acs.inorgchem.6b00017

Peer reviewed

Structure and Reactivity of X-ray Amorphous Uranyl Peroxide, U_2O_7

Samuel O. Odoh,[†] Jacob Shamblin,[‡] Christopher A. Colla,[§] Sarah Hickam,^{||} Haylie L. Lobeck,^{||} Rachel A. K. Lopez,^{||} Travis Olds,^{||} Jennifer E. S. Szymanowski,^{||} Ginger E. Sigmon,^{||} Joerg Neufeind,[⊥] William H. Casey,[§] Maik Lang,[‡] Laura Gagliardi,[†] and Peter C. Burns^{*,||,‡}

[†]University of Minnesota, Department of Chemistry, Minnesota Supercomputing Institute, Minneapolis, Minnesota 55455, United States

[‡]Department of Nuclear Engineering, University of Tennessee, Knoxville, Tennessee 37996, United States

[§]Department of Earth and Planetary Sciences, Department of Chemistry; University of California, Davis, California 95616, United States

^{||}Department of Civil and Environmental Engineering and Earth Sciences, University of Notre Dame, Notre Dame, Indiana 46556, United States

[⊥]Chemical and Engineering Materials Division, Oak Ridge National Laboratory, Oak Ridge, Tennessee 37831, United States

[#]Department of Chemistry and Biochemistry, University of Notre Dame, Notre Dame, Indiana 46556, United States

Supporting Information

ABSTRACT: Recent accidents resulting in worker injury and radioactive contamination occurred due to pressurization of uranium yellowcake drums produced in the western U.S.A. The drums contained an X-ray amorphous reactive form of uranium oxide that may have contributed to the pressurization. Heating hydrated uranyl peroxides produced during *in situ* mining can produce an amorphous compound, as shown by X-ray powder diffraction of material from impacted drums. Subsequently, studtite, $[(UO_2)(O_2)(H_2O)_2](H_2O)_2$, was heated in the laboratory. Its thermal decomposition produced a hygroscopic anhydrous uranyl peroxide that reacts with water to release O_2 gas and form metaschoepite, a uranyl-oxide hydrate. Quantum chemical calculations indicate that the most stable U_2O_7 conformer consists of two bent $(UO_2)^{2+}$ uranyl ions bridged by a peroxide group bidentate and parallel to each uranyl ion, and a μ_2 -O atom, resulting in charge neutrality. A pair distribution function from neutron total scattering supports this structural model, as do 1H - and ^{17}O -nuclear magnetic resonance spectra. The reactivity of U_2O_7 in water and with water in air is higher than that of other uranium oxides, and this can be both hazardous and potentially advantageous in the nuclear fuel cycle.



INTRODUCTION

Accidents resulting from pressurization of drums of uranium yellowcake produced in the western U.S.A. have resulted in worker injury and contamination.¹ While examining the contents of a drum that was involved in one such accident on September 9, 2014 in Metropolis, Illinois, we identified a reactive and poorly understood amorphous uranium oxide peroxide compound. During uranium recovery by *in situ* leaching in the western U.S.A. and elsewhere, uranyl peroxides are precipitated from water by addition of hydrogen peroxide, followed by heating to remove some or all of the water, resulting in lower hydrates of uranyl peroxide or various uranium oxides, depending on the maximum temperature and duration. According to the U.S. Nuclear Regulatory Commission (NRC) and consistent with an earlier study, pressurization of drums of yellowcake can be caused by O_2 gas released during decomposition of yellowcake formed by hydrogen-peroxide precipitation.^{1,2} The potential importance of uranium compounds produced by heating uranyl peroxides has inspired our

attempts to understand the structure and reactivity of such materials.

The interaction of peroxide with the uranyl moiety, $(UO_2)^{2+}$, is stronger than other inorganic ligands,^{3,4} and the nanoscale chemistry of uranyl peroxides has been developed rapidly over the past decade.^{5,6} Discovered in 2005, water-soluble nanoscale uranyl-peroxide cages self-assemble in water.^{5,6} In contrast, stable water-insoluble hydrated uranyl peroxides, first noted in 1876, form when hydrogen peroxide is added to uranyl-bearing water. They are commonly used to control the speciation, solubility, and oxidation states of actinides in the fuel cycle, and for recovery of uranium in *in situ* leaching operations. The two hydration states, $[(UO_2)(O_2)(H_2O)_2](H_2O)_2$ and $[(UO_2)(O_2)(H_2O)_2]$, known as studtite and metastudtite, respectively, occur naturally due to the buildup of peroxide formed by radiolysis of water.⁷ In each, uranyl ions are bridged through

Received: January 4, 2016

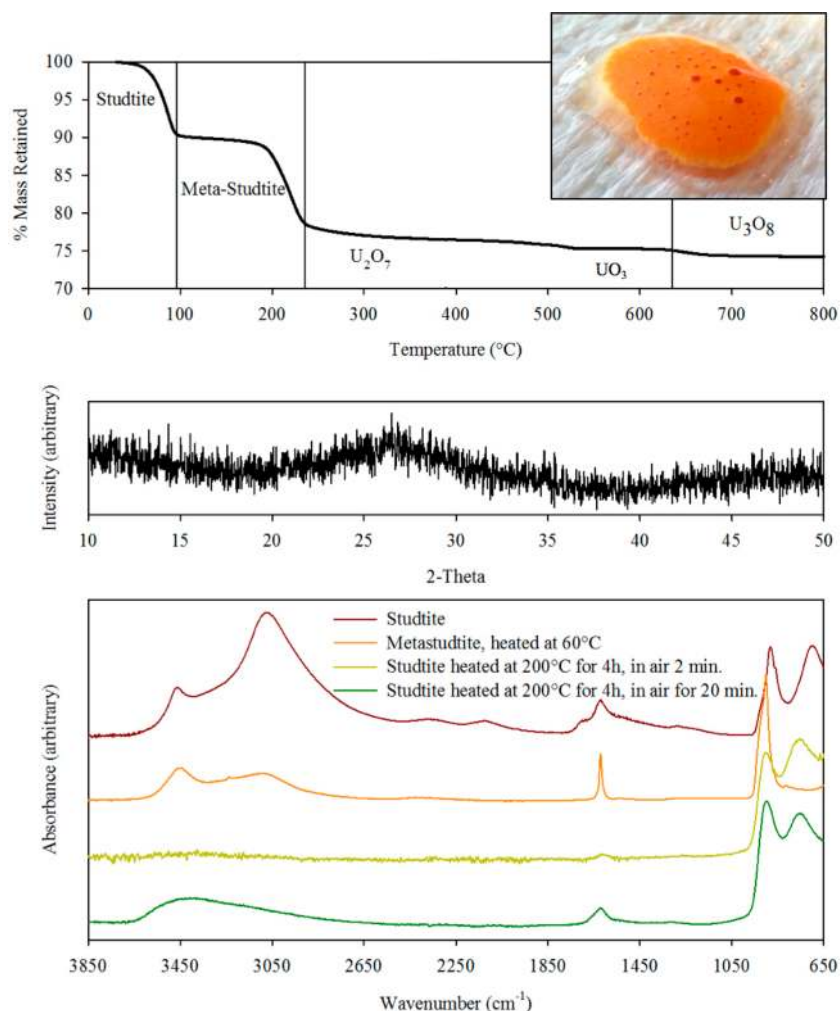
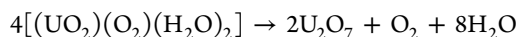


Figure 1. Characterization of *am*-U₂O₇ (details in the SI). (top) Thermogravimetric analysis starting with synthetic studtite, [(UO₂)(O₂)(H₂O)₂]- (H₂O)₂ done by heating at 10 °C/minute in air. (middle) X-ray powder diffractogram of *am*-U₂O₇ formed by heating synthetic metastudtite to 200 °C for one hour. (bottom) Infrared spectra for dried *am*-U₂O₇ produced by heating at 200 °C for four hours in air, *am*-U₂O₇ exposed to air for 20 min under ambient conditions, studtite, and metastudtite. The photo inset shows the reaction of *am*-U₂O₇ with water to release O₂ gas.

bidentate peroxide groups to form chains.^{8,9} They crystallize where high radiation fields cause radiolysis of water, such as on Chernobyl “lava” from the 1986 accident,¹⁰ in irradiated fuel cooling pools, where water contacts irradiated fuel in the laboratory,¹¹ and potentially in the damaged nuclear reactor cores at Fukushima^{12,13} and in a geological repository for nuclear waste.¹⁴

Boggs and El-Chehabi² reported in 1957 that heating metastudtite in air results in the loss of half of the peroxide and all of the water, giving the orange compound U₂O₇ by the reaction:



The rate of this reaction was found to depend strongly on temperature. Boggs and El-Chehabi found that U₂O₇ reacts upon contact with water and releases O₂ gas.² Such a reaction is a potential cause of pressurization of drums containing yellowcake. Boggs and El-Chehabi did not report X-ray data for U₂O₇. However, in a study reported in 1961, orange powders obtained upon dehydration of metastudtite at 400 °C were found to be X-ray amorphous, and were assumed to have composition UO₃.¹⁵ In the same year, Sato demonstrated that the dehydration product of metastudtite formed at 200 °C was

X-ray amorphous, and concluded it corresponds to a form of hydrated UO_x (3 ≤ x ≤ 3.5).¹⁶ Much more recently, the dehydration of metastudtite was reported to produce amorphous UO₃·nH₂O.¹⁷ Here we focus on the product of dehydration of metastudtite at 200 °C, its composition and degree of hydration, and the local structure of the X-ray amorphous material. We do this by combining neutron scattering, spectroscopic, and computational approaches.

EXPERIMENTAL SECTION

Synthesis of Studtite and ¹⁷O-Enriched Solids. *Caution:* Uranium is radioactive and should only be handled by individuals who have received training in radiation safety. Studtite, [(UO₂)(O₂)(H₂O)₂]-2H₂O, is readily synthesized in good purity by combining 5 mL of 0.5 M uranyl nitrate solution with 5 mL of 30% hydrogen peroxide in water. Isotopically labeled studtite was synthesized by reacting 5 mL of a 0.5 M ¹⁷O-tagged uranyl nitrate solution with 5 mL of 30% hydrogen peroxide (H₂O₂) in water that had been enriched to 40% in ¹⁷O. The uranyl nitrate had been previously enriched to 40% ¹⁷O in the axial “yl” oxo. This enrichment was accomplished by dissolving uranyl nitrate into 40% H₂¹⁷O followed by illumination overnight with a 300 W UV lamp and crystallization. Success in tagging the uranyl nitrate was confirmed via ¹⁷O NMR. Upon addition of hydrogen peroxide to the uranyl nitrate solution, a cloudy pale yellow precipitate formed

immediately. The suspension was centrifuged for 1 min at 6500 rpm to separate the precipitate from the solution. The chalky pale-yellow solid was placed in a vacuum-desiccator to dry for 48 h. After drying, the identity of the phase was confirmed as studtite by X-ray powder diffraction. The amorphous phases were prepared by heating the isotopically enriched studtite in a platinum crucible at 200 °C (± 5 °C) for 1 or 4 h in air. NMR spectra at all steps in the conversion, and with isotopic tags in various positions, were collected at the Keck Solid-State NMR facility at U.C. Davis.

Neutron Scattering Measurements. Structural characterization was performed at the Nanoscale-Ordered Materials Diffractometer (NOMAD) at the Spallation Neutron Source at Oak Ridge National Laboratory. About 100 mg of each sample was measured in 5 mm thin wall precision quartz NMR sample tubes for 36 min at room temperature. NOMAD detectors were calibrated using scattering from diamond powder. In order to obtain the total scattering structure function, $S(Q)$, the sample scattering intensity was normalized to the scattering from a solid vanadium rod and background from an empty NMR tube was subtracted. The PDF was obtained by the Fourier transform of $S(Q)$ with $Q_{\min} = 0.1 \text{ \AA}^{-1}$ and $Q_{\max} = 31.4 \text{ \AA}^{-1}$:

$$G(r) = \frac{2}{\pi} \int_{Q_{\min}}^{Q_{\max}} Q[S(Q) - 1] \sin(Qr) dQ \quad (1)$$

where Q is the scattering vector defined as $Q = 4\pi/\lambda \sin \theta$, and λ and θ are the neutron wavelength and scattering angle, respectively.

Quantum-Mechanical Calculations. Quantum-chemical calculations with density functional theory, DFT,¹⁸ Møller–Plesset second order perturbation theory, MP2,¹⁹ and coupled cluster theory with singles, doubles, and perturbative triple excitations, CCSD(T),²⁰ were used to characterize all possible molecular conformations consisting of two uranyl ions, a peroxide group, and an oxygen atom. The most stable structure was obtained for molecular U_2O_7 optimized with the M06 exchange-correlation functional while describing oxygen atoms with the 6-311++G(3df,3pd) basis set and the uranium atoms with small-core Stuttgart relativistic effective core potentials and associated valence basis sets. Three alternative geometrical structures of molecular U_2O_7 were all found to be at higher energies. This remains the case when we carried out geometry optimizations with 10 other density functionals. These include local functionals: PBE, BLYP, and M06-L; hybrids and meta-hybrids: B3LYP, LC- ω PBE, BHandHLYP, M06-2x, M06-HF; as well as dispersion-corrected functionals: B97D, B3LYP-D3, and LC- ω PBE-D3. The relative energies of the four structures are presented in Table S1 of the Supporting Information (SI). We also carried out geometry optimizations with MP2. Single-point calculations with CCSD(T) were performed on the geometries obtained with the M06 functional.

RESULTS AND DISCUSSION

Powder X-ray diffraction patterns collected for samples of yellowcake taken from the impacted drum at Metropolis, Illinois, revealed the presence of a significant amorphous component, as well as crystalline metastudtite, U_3O_8 , and potentially a trace amount of metaschoepite, a peroxide-free hydrated uranyl oxide with composition $(\text{UO}_3) \cdot \text{H}_2\text{O}$ (Figure S1). As each of these crystalline compounds are known to be stable in water, our attention was subsequently focused on the amorphous material.

We confirmed earlier findings of Boggs and El-Chehabi² by heating studtite and metastudtite at various temperatures and durations in air. Exemplary data are provided in Figure S2, where the conversion of metastudtite powder to an X-ray amorphous material increases with both temperature and time. By 200 °C the transformation to an amorphous material takes place within one hour. Hereafter, this material is designated *am-U₂O₇*.

Thermogravimetric analysis (TGA) at 10 °C per minute starting with synthetic light-yellow studtite produced by

precipitating uranyl from aqueous solution revealed dehydration to metastudtite at ~ 60 °C, and further mass loss at ~ 190 °C for the selected heating rate (Figure 1). X-ray powder diffraction data for the orange powder resulting from heating to 200 °C for an hour show that it is amorphous (Figure 1), and with continued heating TGA and X-ray diffraction showed that it slowly loses mass and converts to crystalline UO_3 near 500 °C. The mass loss starting from studtite or metastudtite indicates that the amorphous material has a composition between UO_4 and UO_3 that is close to U_2O_7 , consistent with the report by Boggs and El-Chehabi designating it as U_2O_7 .² The gradual mass loss in the range of 200 to about 500 °C indicates that the amorphous material exists with a range of compositions or that it is gradually converted to UO_3 .

To probe the presence of water in *am-U₂O₇*, a room temperature infrared spectrum was collected immediately after heating studtite to 200 °C for four hours. This spectrum indicates that the powder is anhydrous (Figure 1), as found in the earlier study.² However, the amorphous material is hygroscopic and absorbs water from air, and the infrared spectrum shows strong H_2O bending and H bonding modes after 20 min of exposure in air (Figure 1). Comparison of the infrared spectrum of air-hydrated *am-U₂O₇* to those of studtite and metastudtite demonstrates that *am-U₂O₇* does not revert to one of these compounds (Figure 1), and X-ray diffraction showed that *am-U₂O₇* left standing in air for several months remains amorphous.

NMR spectra collected for ¹⁷O-labeled studtite, as well as the products of heating this material to 200 °C for various times, provide further insight into the transformation and the composition of the amorphous phase. The NMR spectra exhibit gradual changes over four hours at temperature. The spectra demonstrate dehydration of the material, and the elimination of structural water for the sample that was heated for four hours at 200 °C (Figures S4, S8, and S9), consistent with the observations drawn from the infrared spectra. The NMR spectra also revealed an isotopic scrambling of the oxide sites (Figures S4, S8, and S9). ¹H- and ¹⁷O CP-NMR spectra for *am-U₂O₇* exposed to air show signals consistent with structural water and a $\mu\text{-OH}$ site (Figures S11 and S12), consistent with the hygroscopic behavior revealed by infrared spectroscopy.

The infrared vibrational spectrum of *am-U₂O₇* only contains peaks attributable to symmetric and antisymmetric stretching of uranyl ions. The ¹⁷O NMR spectra for *am-U₂O₇* prepared from uranyl and water that were both enriched in ¹⁷O show axial “yl” oxygen in the uranyl ions. The same NMR spectra also contain peaks in the 200–500 ppm range, and these are consistent with bridging oxo derived from water, since the oxygen in the peroxide was not isotopically tagged (SI).

Addition of liquid water to *am-U₂O₇* causes an immediate reaction with release of substantial O_2 gas and conversion of the orange *am-U₂O₇* to a bright yellow solid over the course of a few minutes (Figure 1). This observation is consistent with the earlier findings of Boggs and El-Chehabi, who captured 94% of the evolved oxygen expected when U_2O_7 was added to dilute sulfuric acid.² Our powder X-ray diffraction data for *am-U₂O₇* reacted with water show that the resulting yellow solid is well-crystallized metaschoepite, a uranyl oxide hydrate that contains no peroxide (SI).

The evolved O_2 gas is attributed to the breakdown of peroxide during conversion of *am-U₂O₇* to metaschoepite. NMR spectra collected for metaschoepite prepared in this way

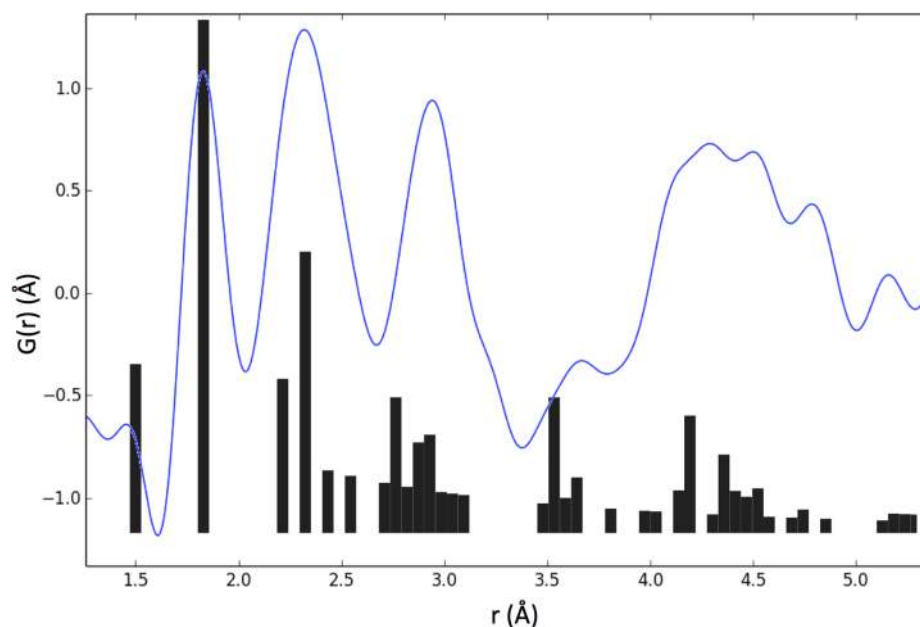


Figure 2. Pair distribution function (PDF) (blue line) derived from neutron scattering data collected at the Spallation Neutron Source (SNS) for *am*-U₂O₇. The black bars indicate atom-atom correlations in the optimized model structure (shown in Figure 4c), with their height proportional to the frequency of the correlation. $O_{\max} = 31.414 \text{ \AA}^{-1}$.

from ¹⁷O-bearing *am*-U₂O₇ revealed scrambling of ¹⁷O among oxide sites (Figure S15), such that the resulting metaschoepite has ¹⁷O in all oxide sites, although the initial studdite and *am*-U₂O₇ were not fully tagged (Figures S19 and S20).

Given that *am*-U₂O₇ is X-ray amorphous, very little information about its structure can be derived from conventional diffraction studies. In order to gain information on the local structure of *am*-U₂O₇, we collected neutron-scattering data for dry *am*-U₂O₇ at the NOMAD beamline of the Spallation Neutron Source (SNS, Oak Ridge National Laboratory). These data provided a pair-distribution function (PDF, Figure 2). In contrast to X-ray scattering, which would mostly reflect the positions of the uranium atoms because of their high scattering efficiency, neutron scattering is also sensitive to the oxygen atoms. The presence of several peaks in the neutron PDF reveals that there is significant local order in *am*-U₂O₇, but only to $\sim 5.5 \text{ \AA}$, consistent with its X-ray amorphous average structure. The PDF correlations at ~ 1.5 and 1.8 \AA confirm the presence of peroxide and uranyl ions, respectively, as peroxide O—O and uranyl U(VI)—O bond lengths are about 1.45 and 1.79 \AA , respectively. Correlations at $\sim 2.3 \text{ \AA}$ arise from the uranyl-ion equatorial-coordination environment, and are consistent with typical U(VI)—O equatorial bond lengths in peroxides.^{6,8} Correlations at larger distances are due to nonbonding separations. The PDF represents an average of configurations, but the degree of local order at distances less than $\sim 5.5 \text{ \AA}$ indicates that a small number of local configurations are dominant in the amorphous material.

Our spectroscopic, thermogravimetric, and neutron scattering experiments, taken together, indicate that *am*-U₂O₇ is a hygroscopic anhydrous uranyl peroxide compound that produces atom-atom correlations to $\sim 5.5 \text{ \AA}$ in the PDF, that reacts with water to release O₂ gas and produce solid metaschoepite, and that is X-ray amorphous. The electro-neutrality requirement restricts the composition to approx-

imately (UO₂)₂(O₂)O, where (O₂) designates a peroxide group having a formal charge of -2 .

Those U₂O₇ species favored by our calculations are designated A through D (Figure 3). Initial trial structures

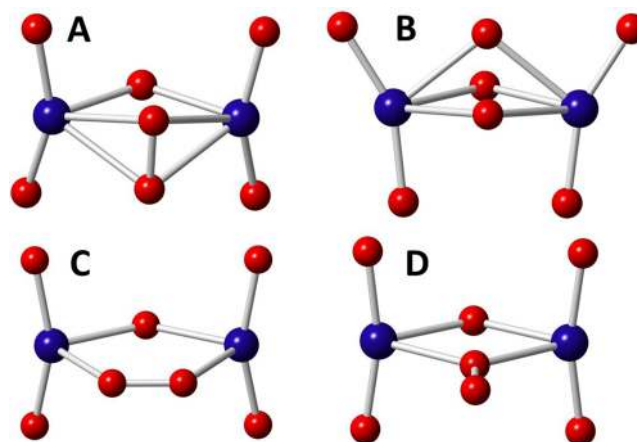


Figure 3. Model structures of U₂O₇ optimized with the M06 density functional. These structures contain a peroxide group, an μ^2 -O and two uranyl moieties.

with other configurations, such as those in which an oxygen atom of one uranyl ion coordinates a second uranyl ion, invariably optimized to one of A–D and thus our attention is hereafter focused on these local configurations. We explored the relative stabilities of A–D with several types of exchange-correlation density functionals as well as with MP2, and CCSD(T) (SI). Regardless of the level of the theory, A is predicted to be the lowest energy structure. Optimized geometrical parameters of this conformer obtained with the M06²¹ density functional are reported in Figure 4.

Species A, which we calculate is the lowest energy species with composition U₂O₇, contains two bent uranyl ions bridged

by a bidentate peroxide group aligned approximately parallel to the uranyl ions, and by a single μ_2 -O atom (Figure 4). Species

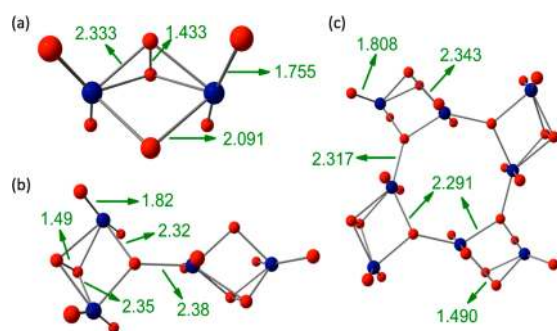


Figure 4. Preferred model structure of U_2O_7 , with U and O shown in blue and red, respectively. All bond distances are given in Å. In (a), we present an isolated U_2O_7 unit with the bond lengths indicated from the optimized DFT (M06 exchange-correlation functional) structure. In (b), we present a pair of U_2O_7 units interacting through a single O atom, with bond lengths derived by optimizing the geometry against the neutron scattering data. In (c), we present the optimized structure of a cell containing four U_2O_7 units interacting through their single O atoms. The calculated structural parameters are in good agreement with the experimental neutron scattering data.

C, which is predicted to have an energy that is closest to that of A, incorporates an end-on peroxide-uranyl configuration. Many compounds contain peroxide that is bidentate to uranyl, although with the peroxide group perpendicular to the uranyl ion, but none are known to contain peroxide end-on coordination to uranyl as in species C. The energy difference between A and C (9.3 kcal/mol with the BLYP^{21,22} functional and up to 13.0 kcal/mol with CCSD(T)) indicates that $am-U_2O_7$ will be dominated by A, with potentially lesser quantities of the other species also present. Species B and D are predicted to be much higher in energy (50–95 kcal/mol for B and 28–49 kcal/mol for D) with DFT, MP2, and CCSD(T). In species B, a peroxide group is perpendicular to the two uranyl ions that it bridges. Although this is the most common configuration of peroxide in uranyl compounds, in this case there is little room left for the bridging oxygen, which destabilizes the configuration.

The PDF calculated for species A using the optimized bond lengths obtained from the DFT calculations is in overall agreement with the PDF derived from the neutron scattering data, with the notable exception of the lack of a correlation at 2.09 Å in the observed PDF, and several correlations in the range of 4.0 to 5.5 Å in the experimental data that are not predicted by the model because it is too small. The optimized structure of A contains an μ_2 -O atom that bridges the uranyl ions at a distance of 2.09 Å. We hypothesize that this μ_2 -O atom interacts with an adjacent U_2O_7 species, coordinating a uranyl ion on the side opposite the peroxide group (Figure 4b). The ring structure shown in Figure 4c permits each μ_2 -O to become μ_3 -O, and has been optimized by using the PBE²³ exchange-correlation functional. This ring structure is a tetramer of U_2O_7 with composition U_8O_{28} . After geometry optimization, interactions between adjacent U_2O_7 units give μ_3 -O atoms with bonds to U(VI) at typical values of ~ 2.3 Å, and produce correlations in the range of 4.0 to 5.5 Å. The overall PDF calculated for the DFT-optimized structure of four-membered rings of U_2O_7 is compared to that from neutron scattering in Figure 2, where good correspondence is observed.

We therefore propose that species A, arranged in various ways, corresponds to a substantial portion of $am-U_2O_7$.

CONCLUSIONS

Here we have confirmed that $am-U_2O_7$ is anhydrous and contains peroxide, that its reaction with water results in release of oxygen, and that the reaction scrambles isotopic tags in the various oxide sites. Our study is the first to attempt to determine the local structure of $am-U_2O_7$, which is a difficult problem owing to the lack of long-range order amenable to diffraction studies. We have combined neutron scattering, infrared, and nuclear magnetic resonance spectroscopies including isotopic labels, and high-level computational approaches to provide insight into the local structure of $am-U_2O_7$ and the reasons why it is reactive with water. Formation of $am-U_2O_7$ from metastudtite is a kinetically controlled process that warrants additional detailed study. It is possible that metastudtite contained in yellowcake gradually converts to $am-U_2O_7$ at room temperature or under elevated storage temperatures, and that $am-U_2O_7$ may in turn decompose to release oxygen gas. Given the potential importance of this process during the shipment and storage of yellowcake, we plan further studies to define the time–temperature dependence of conversion.

Uranium oxides including UO_2 , U_3O_8 , and the various polymorphs of UO_3 are generally unreactive in water, in contrast to $am-U_2O_7$. The reactivity of $am-U_2O_7$ in water is attributable to the strained configuration of the uranyl ion, the amorphous state, and the presence of peroxide that can be liberated. $am-U_2O_7$ may have important applications in an advanced nuclear fuel cycle, such as in hydro-fluorination reactions for a more environmentally sustainable method for production of UF_6 . Formation of reactive $am-U_2O_7$ during uranium yellowcake preparation, treatment, storage, or transport may be a contributing factor in drum pressurization incidents that have been documented repeatedly by the US NRC.¹ Although we have identified an amorphous phase among the contents of a drum of yellowcake that was found to be pressurized, it is currently impossible to specify the cause of the various instances of yellowcake drum pressurization.

ASSOCIATED CONTENT

Supporting Information

The Supporting Information is available free of charge on the ACS Publications website at DOI: 10.1021/acs.inorgchem.6b00017.

X-ray powder diffraction data, NMR spectra, TGA curves, IR spectra, photographs, and details of quantum mechanical calculations (PDF)

AUTHOR INFORMATION

Corresponding Author

*E-mail: pburns@nd.edu (P.C.B.)

Notes

The authors declare no competing financial interest.

ACKNOWLEDGMENTS

This research is funded by the Office of Basic Energy Sciences of the U.S. Department of Energy as part of the Materials Science of Actinides Energy Frontier Research Center (DE-SC0001089). Chemical analyses were conducted at the Center for Environmental Science and Technology at the University of

Notre Dame. Spectra and diffraction data were collected at the Materials Characterization Facility of the Center for Sustainable Energy at the University of Notre Dame. A portion of this research at ORNL's Spallation Neutron Source was sponsored by the Scientific User Facilities Division, Office of Basic Energy Sciences, US Department of Energy. The authors thank Dr. Ping Yu of the UC Davis Keck NMR Facility for help with the NMR spectra.

REFERENCES

- (1) U.S. Nuclear Regulatory Commission. *Exothermic reactions involving dried uranium oxide powder (yellowcake)*, 2014.
- (2) Boggs, J. E.; Elchehabi, M. J. *J. Am. Chem. Soc.* **1957**, *79*, 4258–4260.
- (3) Vallet, V.; Wahlgren, U.; Grenthe, I. J. *J. Phys. Chem. A* **2012**, *116*, 12373–12380.
- (4) Odoh, S. O.; Schreckenbach, G. *Inorg. Chem.* **2013**, *52*, 5590–5602.
- (5) Burns, P. C.; Kubatko, K. A.; Sigmon, G.; Fryer, B. J.; Gagnon, J. E.; Antonio, M. R.; Soderholm, L. *Angew. Chem., Int. Ed.* **2005**, *44*, 2135–2139.
- (6) Qiu, J.; Burns, P. C. *Chem. Rev.* **2013**, *113*, 1097–1120.
- (7) Kubatko, K. A. H.; Helean, K. B.; Navrotsky, A.; Burns, P. C. *Science* **2003**, *302*, 1191–1193.
- (8) Burns, P. C.; Hughes, K. A. *Am. Mineral.* **2003**, *88*, 1165–1168.
- (9) Weck, P. F.; Kim, E.; Jove-Colon, C. F.; Sassani, D. C. *Dalton Trans.* **2012**, *41*, 9748–9752.
- (10) Burakov, B. E.; Strykanova, E. E.; Anderson, E. B. *In Scientific Basis for Nuclear Waste Management Xx*; Gray, W. J., Triay, I. R., Eds. **1997**; Vol. 465, p 1309-1315.
- (11) Hanson, B.; McNamara, B.; Buck, E.; Friese, J.; Jenson, E.; Krupka, K.; Arey, B. *Radiochim. Acta* **2005**, *93*, 159–168.
- (12) Armstrong, C. R.; Nyman, M.; Shvareva, T.; Sigmon, G. E.; Burns, P. C.; Navrotsky, A. *Proc. Natl. Acad. Sci. U. S. A.* **2012**, *109*, 1874–1877.
- (13) Burns, P. C.; Ewing, R. C.; Navrotsky, A. *Science* **2012**, *335*, 1184–1188.
- (14) Shuller-Nickles, L. C.; Bender, W. M.; Walker, S. M.; Becker, U. *Minerals* **2014**, *4*, 690–715.
- (15) Hoekstra, H. R.; Siegel, S. J. *J. Inorg. Nucl. Chem.* **1961**, *18*, 154–165.
- (16) Sato, T. *Naturwissenschaften* **1961**, *48*, 693–693.
- (17) Guo, X.; Ushakov, S. V.; Labs, S.; Curtius, H.; Bosbach, D.; Navrotsky, A. *Proc. Natl. Acad. Sci. U. S. A.* **2014**, *111*, 17737–17742.
- (18) Capelle, K. *Braz. J. Phys.* **2006**, *36*, 1318–1343.
- (19) Møller, C.; Plesset, M. S. *Phys. Rev.* **1934**, *46*, 618–622.
- (20) Raghavachari, K.; Trucks, G. W.; Pople, J. A.; Headgordon, M. *Chem. Phys. Lett.* **1989**, *157*, 479–483.
- (21) Becke, A. D. *Phys. Rev. A: At., Mol., Opt. Phys.* **1988**, *38*, 3098–3100.
- (22) Lee, C. T.; Yang, W. T.; Parr, R. G. *Phys. Rev. B: Condens. Matter Mater. Phys.* **1988**, *37*, 785–1988.
- (23) Perdew, J. P.; Burke, K.; Ernzerhof, M. *Phys. Rev. Lett.* **1996**, *77*, 3865–3868.